

Chemical doping and intergranular magnetic-field effects in bulk thallium-based superconductors

M. Yang* and Y. H. Kao

Department of Physics, State University of New York at Buffalo, Amherst, New York 14260

Y. Xin and K. W. Wong

Department of Physics and Astronomy, University of Kansas, Lawrence, Kansas 66045

(Received 30 June 1994)

Measurements of ac magnetic susceptibility of bulk $\text{Tl}_2\text{Ba}_2\text{Ca}_2\text{Cu}_3\text{O}_y$ and compounds containing noble-metal additives were carried out to investigate the effects of chemical doping and penetration of magnetic field into the intergranular region. Significant enhancement of the intergranular critical current density was demonstrated in Tl-based ceramic superconductors with Au and Ag doping. Methods for convenient determination of the intergranular weak-link phase-locking temperature and average lower critical field in the bulk granular superconductors are discussed.

I. INTRODUCTION

It is well known that large-scale applications of high-temperature superconductors (HTS's) are severely limited at the present stage because of the difficulty of low transport critical current in the bulk material. Ceramic HTS's usually consist of agglomerates of anisotropic grains separated by nonstoichiometric interfacial materials and show a precipitous decrease of transport critical current density J_c in low magnetic fields. This behavior of J_c can be mainly attributed to the Josephson-type weak links (WL's) formed between the superconducting grains, which are sensitive to the local magnetic flux and can only support a low *intergranular* supercurrent. Physical studies of the temperature and magnetic field dependence of J_c are important not only for technical applications, but also to provide information on the distribution of magnetic flux lines in these bulk granular superconductors (BGS's).¹

Among the known techniques for probing the magnetic structures in BGS's, ac magnetic susceptibility is uniquely suited for this purpose because of its high sensitivity to the effects of *low* magnetic fields. Earlier studies^{2,3} using this method have already revealed much useful information. Measurements of the ac susceptibility $\chi = \chi' + i\chi''$ in an applied magnetic field $H(t) = H_{dc} + H_{ac} \cos \omega t$ generally show features of two steps in the in-phase component χ' and two peaks in the out-of-phase component χ'' . However, most of the previous experiments⁴⁻⁹ on *low-field* susceptibility appeared to focus mainly on measurements with an applied *ac* field; effects arising from a *variable dc* magnetic field have thus far not been well explored.

In this paper, we report recent studies of the ac magnetic susceptibility in pure, Ag-doped, and Au-doped $\text{Tl}_2\text{Ba}_2\text{Ca}_2\text{Cu}_3\text{O}_y$ BGS's as a function of temperature using *both ac* and *dc* magnetic fields. A new method for *direct* determination of the phase-locking temperature T_{cJ} (J for Josephson coupling) pertaining to coherent WL's has been found. This temperature is closely related

to the intergranular (or transport) critical current of BGS's. The effects of an applied *dc* magnetic field are compared with theoretical calculations based on the Anderson-Kim model.¹⁰ The changes of *intergranular* local flux density caused by *intragranular* supercurrents are quantitatively investigated. From this study, a new method has also been found for convenient determination of the average lower critical field H_{c1g} of the superconducting grains. Our results show that the WL coupling and intergranular J_c are significantly enhanced by Au or Ag doping in Tl-based BGS's. To the best of our knowledge, this is the first experimental report on susceptibility studies of J_c enhancement in Au- and Ag-doped $\text{Tl}_2\text{Ba}_2\text{Ca}_2\text{Cu}_3\text{O}_y$ as well as the effects of a variable *dc* magnetic field on the pronounced peak in the temperature dependence of the ac magnetic susceptibility.

II. EXPERIMENTAL DETAILS

Susceptibility measurements were performed using a high-sensitivity susceptometer reported elsewhere.¹¹ The inductive and resistive components of the volume susceptibility were measured with a lock-in amplifier at 2 kHz. The effect of frequency variation is negligible in this regime. A high-permeability metal shield was used to provide a well-defined zero-field-cooled condition with a residual field lower than 1 mOe. Temperature changes were made at a rate slower than 0.5 K/min, monitored by a silicon diode sensor. Pure, Ag-doped, and Au-doped $\text{Tl}_2\text{Ba}_2\text{Ca}_2\text{Cu}_3\text{O}_y$ pellets were studied to compare the effects of chemical doping on the pinning force and intergranular J_c . These Tl-based compounds were prepared using a method described elsewhere.¹² The atomic-weight ratio of Au or Ag to $\text{Tl}_2\text{Ba}_2\text{Ca}_2\text{Cu}_3\text{O}_y$ is 1:10 in the doped samples. All samples are single phase, confirmed by x-ray-diffraction measurements. Scanning electron microscope pictures show randomly oriented irregular grains. The grain size ranges between 1.0 and 20 μm , with an average diameter around 4–5 μm . The dimensions of the rectangular-shaped samples are typically 6.0 \times 2.4 \times 0.65

mm.³ The magnetic field was always applied parallel to the longest dimension, and the demagnetization factor is calculated to be lower than 0.05.

III. RESULTS AND DISCUSSION

A typical temperature dependence of the ac susceptibility in zero dc magnetic field is shown in Fig. 1. The most prominent features are the steps in χ' and peaks in χ'' . The temperature at the well-defined peak in χ'' [Fig. 1(a), hereafter called T_{pJ} , clearly shifts to a lower temperature with increasing ac field amplitude H_{ac} , while the weak peak in χ'' at a higher temperature [Fig. 1(b), hereafter called T_{pg} , decreases only slightly with H_{ac} . The inflection points of the large and weak steps in χ' occur at nearly the same temperatures as T_{pJ} and T_{pg} , respectively. It should be noted that these characteristic temperatures T_{pJ} and T_{pg} , owing to their apparent dependence on H_{ac} , are in general lower than the true transition temperature T_c commonly defined at the *onset* of deviation of either χ' or χ'' from the base line. In the samples studied in our experiment, this onset always occurs at the same temperature 120 K, which is defined as the true transition

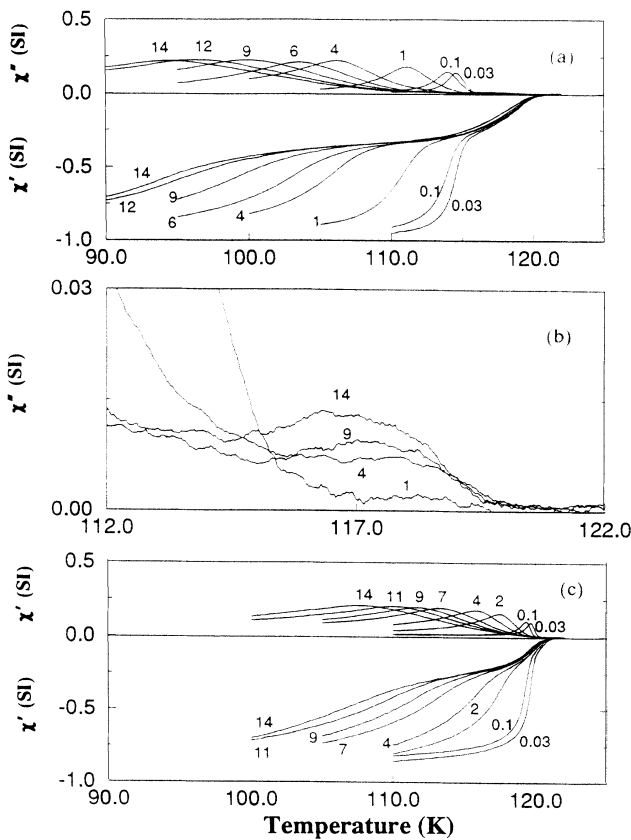


FIG. 1. (a) Experimental data of the ac susceptibility $\chi'(T)$ and $\chi''(T)$ for $\text{Tl}_2\text{Ba}_2\text{Ca}_2\text{Cu}_3\text{O}_y$. Numbers labeling the curves are ac field amplitude H_{ac} in Oe. $H_{dc}=0$. (b) A plot of $\chi''(T)$ in (a) near T_c to reveal the weak peak. (c) Data for a Au-doped sample similar to (a).

temperature T_c of these samples. Variations of T_{pJ} and T_{pg} with H_{ac} are depicted in Fig. 2. Extrapolation of the T_{pg} data to zero magnetic field (shown for the undoped $\text{Tl}_2\text{Ba}_2\text{Ca}_2\text{Cu}_3\text{O}_y$ only) confirms that the intrinsic T_c value for all three samples is indeed 120 K. For the Ag- and Au-doped compounds, T_{pJ} varies linearly with H_{ac} . On the other hand, a slight nonlinearity was found for the undoped sample.

A. Variations of T_{pJ} with chemical doping

Following the procedure described above, an interesting effect clearly appears. The value of T_{pJ} varies with Au and Ag doping. A *direct* plot of T_{pJ} versus H_{ac} gives the intercept of data points on the temperature axis, which can be used as an indicator of the underlying effect of noble-metal doping. The intercept T_{cJ} is defined as the critical temperature for a percolated path of coherent WL's in the BGS due to phase locking between the superconducting grains. For a temperature T below T_{cJ} , the grains are phase locked in the BGS, which can support a bulk supercurrent. A magnetic field H below the lower critical field H_{c1J} of the WL's will induce a screening supercurrent on the outer surface of domains inside the BGS (or the entire BGS) to maintain a state of perfect diamagnetism within these domains.¹¹ T_{cJ} is proportional to the average coupling energy between the phase-locked grains; hence, it serves as a measure of the supercurrent that can be sustained by the coherent BGS. Above this temperature, complete phase coherence between the superconducting grains is broken; an external magnetic field can then enter the intergranular region, although each grain may still maintain its own Meissner state. Since the transport critical current is proportional to the minimum Josephson-type intergrain coupling energy in a

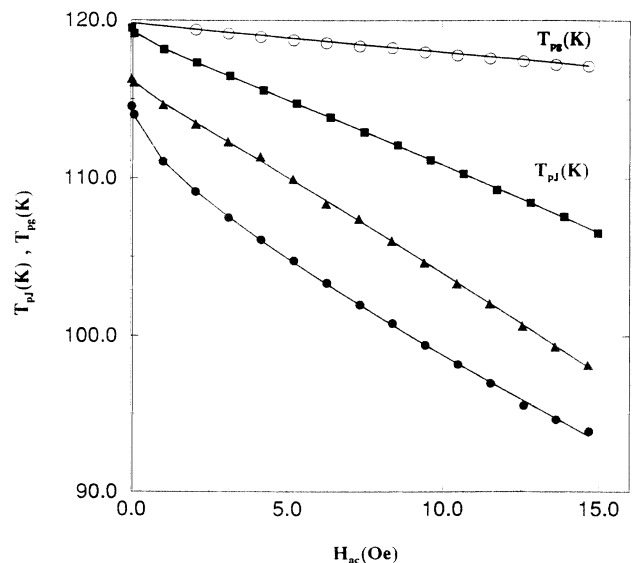


FIG. 2. Temperature at the pronounced peak T_{pJ} as a function of ac field amplitude H_{ac} for the undoped (\bullet), Ag-doped (\blacktriangle), and Au-doped (\blacksquare) samples. Temperature dependence of T_{pg} at the weak peak for the undoped sample is also shown (\circ).

BGS, a higher value of T_{cJ} therefore implies a higher transport J_c .

From the intercept, as shown in Fig. 2, T_{cJ} can be directly determined without any curve-fitting or adjustable parameters. By this method, T_{cJ} is found to be 114.56, 116.44, and 119.55 K for the undoped and Ag- and Au-doped samples, respectively. We have thus demonstrated that Ag and Au doping can lead to a significant enhancement of T_{cJ} (or intergranular/transport J_c) in TI-based BGS's.

B. Effects of a variable low magnetic field

The temperature dependence of the ac susceptibility in a low dc magnetic field H_{dc} is shown in Fig. 3(a). Although the main features look similar to those in Fig. 1, the net effect of a dc magnetic field is actually quite different. An applied H_{dc} much higher than H_{ac} is required to shift T_{pJ} by the same amount. The dependence of T_{pJ} on H_{dc} for the undoped and Au-doped samples is

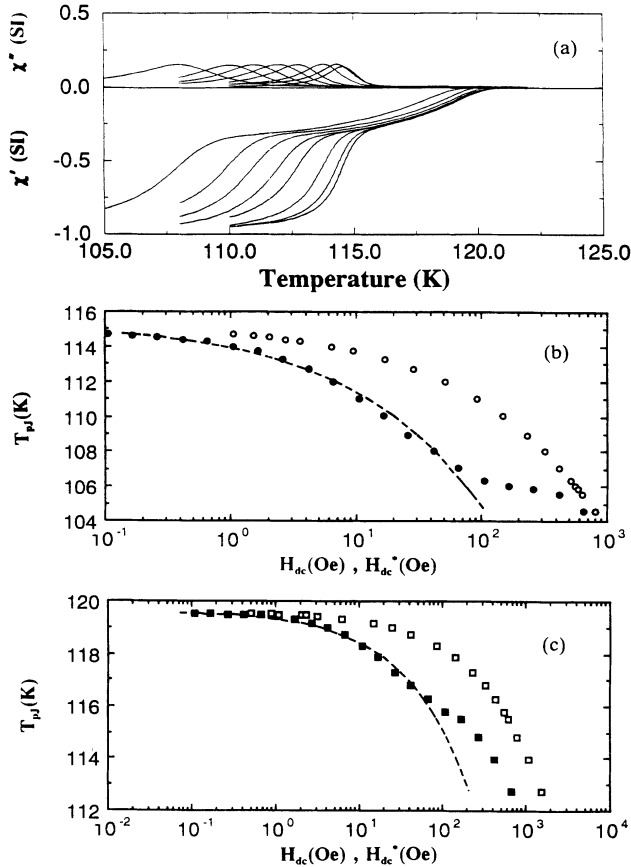


FIG. 3. (a) Experimental data of the ac susceptibility $\chi'(T)$ and $\chi''(T)$ for $Tl_2Ba_2Ca_2Cu_3O_y$ in a dc magnetic field H_{dc} . The ac field amplitude is kept constant at $H_{ac}=0.03$ Oe. $H_{dc}=0.16, 0.63, 1.58, 4.0, 6.3, 10.0, 15.8$ and 39.8 Oe for the curves from right to left. (b) Variations of T_{pJ} as a function of applied dc field H_{dc} (●) and calculated field value (○) H_{dc}^* derived from Eq. (8). The dashed curve is a plot of T_{pJ} vs $H_{dc}^*/7.5$. (c) Plots for a Au-doped sample similar to (b) except for a different scaling factor of 7.25 for H_{dc}^* .

shown in Figs. 3(b) and 3(c), respectively. Similar behavior was also found with the Ag-doped sample (not shown in the figure). It is interesting to note that T_{pJ} follows a smooth variation with H_{dc} [see dashed curves in Figs. 3(b) and 3(c)] until a *kink* appears around 70 Oe. As will be discussed in the following, these observations provide useful information on the intergranular field distribution and also allow a convenient method to determine the average lower critical field H_{c1g} of the superconducting grains.

These results can be understood in terms of field penetration into the BGS in conjunction with the Anderson-Kim critical state model¹⁰ and Clem's model¹³ of BGS's. The ratio of the Josephson coupling energy to the intragranular condensation energy is on the order of 10^{-8} ; hence, a weakly coupled grain model¹³ should hold over a wide temperature range up to the vicinity of T_c . In an H between H_{c1J} and H_{c1g} , the field penetrates the intergranular region into a depth λ_J , much deeper than into the grains; the BGS may thus be approximated by a homogeneous medium. By a comparison of our data with theoretical calculations based on these established models, much useful information about the field distribution inside the BGS can be derived from the observed variations of the shape and position of the ac susceptibility peaks.

C. Model calculations (without a dc magnetic field)

We calculated $\chi(T)$ in an applied field $H(t)=H_{dc}+H_{ac}\cos\omega t$ in a way similar to Müller's theoretical work,⁴ but with appropriately modified expressions in order to account for our new experimental observations. The BGS is considered in the shape of an infinitely large thin slab with thickness $2d$ in the x direction. To include the size effect of the grains, we assumed an approximation after Clem's model in which the grains are represented by a random distribution of superconducting cylinders, each of radius R_g and with its axis parallel to the magnetic field along the z axis. This approximation, though not entirely realistic, at least allows a tractable calculation to account for the gross features of various grain sizes with an *average* radius equal to R_g . Depending on the pinning force, intergranular vortices may move when $H(t)$ exceeds H_{c1J} . The flux density can be expressed as $B=\mu_{eff}H$; here, $\mu_{eff}(T)$ is an effective permeability of the BGS as given also by Müller [see Eq. (4) in Ref. 4]. The local inter- and intragranular magnetic fields $H_J(x,t)$ and $H_g(r,x,t)$ can be obtained from the critical state equations

$$\frac{dH_J(x,t)}{dx} = \pm J_{cJ}(x,t), \quad (1)$$

$$\frac{dH_g(r,x,t)}{dr} = \pm J_{cg}(r,x,t), \quad (2)$$

in conjunction with expressions in the Anderson-Kim model¹⁰ for the local inter- and intragranular critical current densities:

$$J_{cJ}(x, t) = \frac{\alpha_J(T)}{\mu_{\text{eff}}\mu_0} \frac{1}{|H_J(x, t)| + H_{0J}}, \quad (3)$$

$$J_{cG}(r, x, t) = \frac{\alpha_g(T)}{\mu_0} \frac{1}{|H_g(r, x, t)| + H_{0g}}. \quad (4)$$

Here the \pm signs correspond to the motion of vortices in decreasing or increasing applied field, α_J and α_g are the respective pinning force densities¹⁰ (assumed to be independent of H in the low-field regime), and H_{0J}, H_{0g} are positive parameters.

The following form of the temperature dependence was used to determine $J_{cJ}(T)$:

$$\alpha_J(T)/\mu_{\text{eff}}(T) = [\alpha_J(0)/\mu_{\text{eff}}(0)](1 - T/T_{cJ})^n. \quad (5)$$

This expression is different from that used by Müller in two respects. We have replaced T_c by T_{cJ} to account for our observed changes in T_{cJ} for the coherent WL's in the

$$H_{ac} = H^*(T_{pJ}) = H_{0J} \{ -1 + [1 + 2\alpha_J(T_{pJ})d/\mu_0\mu_{\text{eff}}(T_{pJ})H_{0J}^2]^{1/2} \}. \quad (6)$$

Likewise, the ac amplitude that yields a peak at T_{pg} is given by $H^*(T_{pg})$ in the following:

$$H_{ac} = H^*(T_{pg}) = H_{0g} \{ -1 + [1 + 2\alpha_g(T_{pg})R_g/\mu_0H_{0g}^2]^{1/2} \}, \quad (7)$$

when the applied field has just reached the center of the "cylindrical grains" ($r=0$).

Typical results of our model calculations using Eqs. (6) and (7) for the temperature dependence of χ' and χ'' in the absence of a dc magnetic field are shown in Figs. 4(a) and 4(b). The curves shown in Fig. 4(a) are in good agreement with our experimental data [e.g., Fig. 1(a)]. By a comparison, the relevant parameters $\alpha_J(0)$ and H_{0J} were determined, and the intergranular critical current density J_{cJ} can be deduced from Eqs. (3) and (5). The obtained parameters are $\alpha_J(0) = 6.5 \times 10^4$, 3.1×10^4 , 4.8×10^4 TA m⁻²; $H_{0J} = 0.194$, 0.096 , and 0.190 mT; J_{cJ} (at 77 K) = 6.8×10^3 , 1.35×10^4 , and 1.51×10^4 A cm⁻²; and the maximum critical current $I_0(0) = 49$, 62 , and 503 μ A for the undoped and Ag- and Au-doped Tl₂Ba₂Ca₂Cu₃O_y samples, respectively. For Ag- and Au-doped BGS's the exponent n in (5) is equal to 2, indicating the presence of SNS-type WL's. Hence noble-metal doping mainly results in an enhanced $I_0(0)$ with only a minor change in the intergranular pinning force density $\alpha_J(0)$. These observations of J_{cJ} enhancement and pinning force density could be useful for technical applications of BGS's.

It should be noted that the height of peaks in $\chi''(T)$ depends on the radius of the superconducting grains [see Fig. 4(b)]. By a comparison with the data, the *average* radius of grains in our samples is found to be around 2μ m, which can be compared with the average grain size of 4 – 5μ m diameter observed by scanning electron microscopy (SEM). This method affords a convenient *nondescriptive determination of average grain size* in bulk HTS's.

We compared the intergranular J_c deduced from the

BGS, and the exponent n is left as an adjustable parameter to be determined from the experimental data. This modification is necessary because when T approaches T_{cJ} , intergranular vortices can be depinned, and consequently $\alpha_J(T)$ should vanish. The value of n near the transition temperature serves as an indication of the dominant type of WL's present in the BGS. For example, various theoretical models indicate that $n = 1, \frac{3}{2}, 2$ would correspond to Josephson-type, Ginzburg-Landau, and superconducting-normal-superconducting (SNS) weak links, respectively.^{14,15} Spatial and temporal averages of the magnetic inductions were then taken by using Eqs. (1)–(5) to calculate the susceptibilities for comparison with our data.

Detailed numerical calculations indicate that the peak at T_{pJ} in χ'' corresponds almost exactly to a specific condition such that the applied field has just reached the center of the BGS. This specific ac field amplitude $H^*(T_{pJ})$ can be approximated analytically by

susceptibility measurements (which can be regarded as the *intrinsic* intergrain critical current density) with the critical current density obtained from an independent transport measurement. Using a common criterion of an onset current at 1.0μ V/cm, we have determined the values of transport J_c (at 77 K) = 600 , 1400 , and 2100 A cm⁻² for the undoped and Ag- and Au-doped Tl₂Ba₂Ca₂Cu₃O_y compounds, respectively. The transition temperature T_c was found to be also about 120 K. The directly measured transport J_c values are about an order of magnitude lower than the corresponding intrinsic values. Two main factors could probably be responsible for this difference. Joule heating in the WL's during transport measurements could cause a significant decrease in the observed apparent critical current. In contrast, the susceptibility measurements are more sensitive to power loss in the WL's and only a very low probing magnetic field (hence an extremely low induced current) was used in the experiments. Also, the simplifying approximations about regular grains in the BGS assumed in our model calculations, in which the effect of anisotropy was neglected, as well as the deduced average grain size should all be subjected to some corrections.

D. Model calculations (with a variable dc magnetic field)

Following the method discussed in the previous section, similar numerical calculations were carried out to obtain $\chi''(T)$ in a variable dc field H_{dc} under the assumption that $H_{dc} > H_{ac}$. The results are shown in Fig. 4(c), which are in good agreement with our data [e.g., Fig. 3(a)]. As expected, the peak shifts to lower temperature

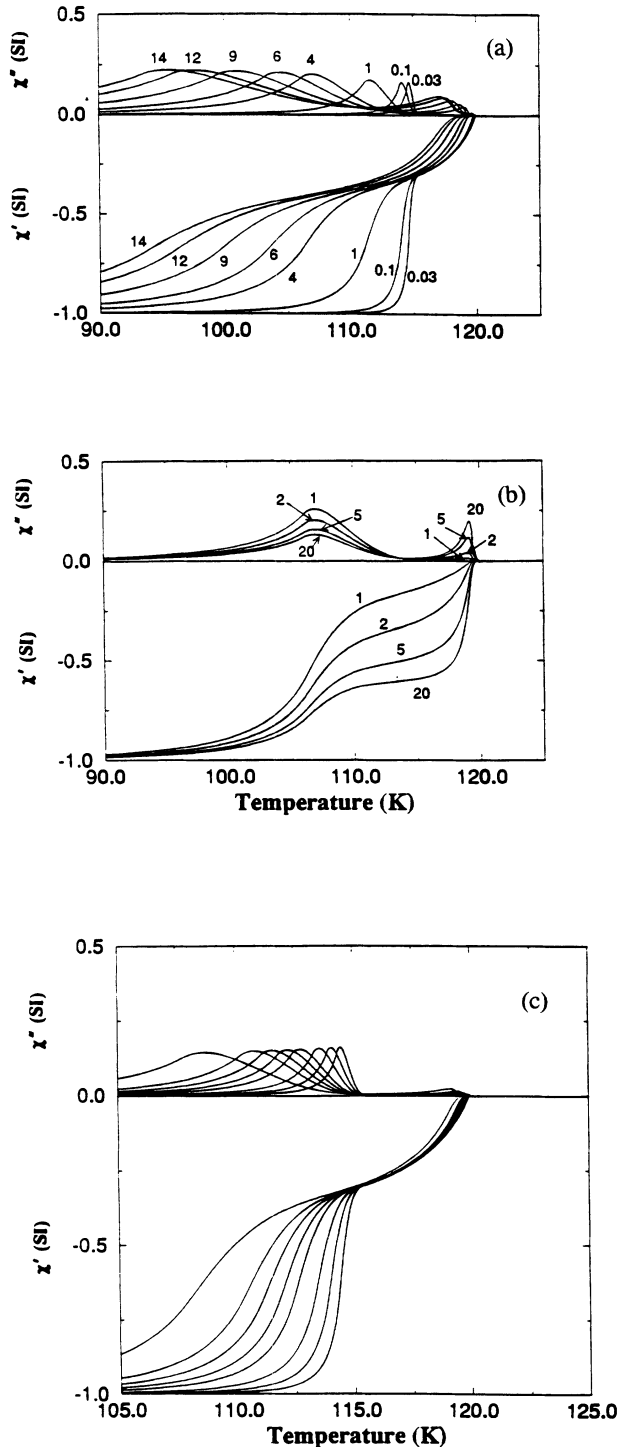


FIG. 4. (a) Calculated ac susceptibility $\chi'(T)$ and $\chi''(T)$ for $\text{Tl}_2\text{Ba}_2\text{Ca}_2\text{Cu}_3\text{O}_y$ with an average grain size $R_g = 2.0 \mu\text{m}$. Numbers labeling the curves are ac field amplitude H_{ac} in Oe. $H_{dc} = 0$. (b) Calculated ac susceptibility $\chi'(T)$ and $\chi''(T)$ for $\text{Tl}_2\text{Ba}_2\text{Ca}_2\text{Cu}_3\text{O}_y$ with various grain sizes. Numbers labeling the curves are values of R_g in μm . Field amplitude $H_{ac} = 4.0$ Oe. $H_{dc} = 0$. (c) Calculated ac susceptibility $\chi'(T)$ and $\chi''(T)$ for $\text{Tl}_2\text{Ba}_2\text{Ca}_2\text{Cu}_3\text{O}_y$ in different dc magnetic fields H_{dc}^* derived from Eq. (8). The ac field amplitude is kept constant at $H_{ac} = 0.03$ Oe. dc field values are $H_{dc}^*/7.5 = 0.16, 0.63, 1.58, 4.0, 6.3, 10.0, 15.8,$ and 39.8 Oe for the curves from right to left.

as H_{dc} is increased. However, the peak position satisfies a specific condition that the total applied field has reached the center ($x=0$) of the BGS and remains stationary there, given by an analytical expression

$$[H_{dc}^*(T_{PJ}) + H_{0J}]H_{ac} = \alpha_J(T_{PJ})d / \mu_0\mu_{\text{eff}}(T_{PJ}). \quad (8)$$

It is interesting to note that the ac field amplitude H_{ac} appears in this expression as a *multiplicative* factor rather than an additive term with H_{dc} . This explains why the effects of the ac susceptibility are so sensitive to H_{ac} , even in the presence of a much higher dc field. Using the values of $\alpha_J(0)$, H_{0J} , T_{cJ} , and n determined before, T_{PJ} and the corresponding dc field H_{dc}^* satisfying Eq. (8) were calculated numerically and plotted as open circles and squares in Figs. 3(b) and 3(c). The calculated values H_{dc}^* are noticeably higher than the actual values of applied dc field (solid circles and squares in the same figures). This difference can be understood in terms of an effect of enhanced intergranular magnetic field discussed in the following.

E. Effect of enhanced intergranular magnetic field

The difference between the calculated H_{dc}^* and actual dc field H_{dc} can be explained by the effect of flux expulsion due to the superconducting grains. When the BGS is cooled in zero field and H_{dc} is below the lower critical field H_{c1g} of the grains, flux expulsion by the grains will cause a *compression* of flux lines in the *intergranular* region, thereby resulting in a higher *local* magnetic flux density. This effect has also been discussed by Evetts and Glowacki¹⁶ and by Levy *et al.*¹⁷ To account quantitatively for this locally enhanced flux density, we have divided the calculated values of H_{dc}^* in Figs. 3(b) and 3(c) by scaling factors of 7.5 and 7.25, respectively, and replotted the down-scaled values of H_{dc}^* as dashed curves in the same figures. The agreement of the rescaled theoretical values with experimental data points is quite good in the region below the kink. The close fits thus indicate that the flux line density in the intergranular region is increased by a factor of about 7.5 before the field could penetrate into the superconducting grains. We therefore identify the value of H_{dc} at the kink as H_{c1g} , which signifies the onset of dc field penetration into the grains. This method suggests a convenient means for a *direct* determination of the average value of H_{c1g} in a BGS.

It should be noted that a low ac amplitude ($H_{ac} = 0.03$ Oe) was used for measuring the ac susceptibility $\chi(T)$ in a variable dc magnetic field as shown in Fig. 3(a). This requirement of low H_{ac} amplitude is essential in order to avoid complications arising from the low-field irreversibility line,¹¹ hysteresis, and disturbance of the order parameter if H_{ac} becomes comparable to H_{c1g} . Also, our method for the determination of T_{cJ} is based on the *low-field* ac susceptibility as a continuous function of temperature. This is different from the method used by Lam and Jeffries.¹⁸ They measured $\chi(T)$ as a function of H_{ac} , which was allowed to exceed H_{c1g} .

The calculated $\chi(T)$ and the peak at T_{PJ} are generally in good semiquantitative agreement with our experimen-

tal results. However, the calculated peak height at T_{pg} is somewhat higher than those measured. This discrepancy is probably due to the fact that thermal fluctuations in the actual experiments and the effects of finite low-field penetration into the grains near the transition temperature were both neglected in the calculations.

IV. CONCLUSIONS

In conclusion, our measurements of the ac susceptibility have revealed new information about the effects of intergranular magnetic field and chemical doping. We have demonstrated a method that can be employed for convenient determination of the coherent phase-locking temperature of coupled weak links in bulk granular su-

perconductors. Au and Ag doping can give rise to significant enhancement of the intergranular critical current density due to the formation of SNS weak links at the grain boundaries. The susceptibility data obtained with both ac and dc magnetic fields are found to be in reasonable quantitative agreement with numerical calculations. Also, a method for determining the average intragranular lower critical field has been found from the variations of a peak with applied dc magnetic field.

ACKNOWLEDGMENTS

The research at SUNY Buffalo was supported in part by the National Science Foundation and by the New York State Institute for Superconductivity. Work at University of Kansas was supported by Midwest Superconductivity, Inc.

*Present address: Yeshiva University, 1300 Morris Park Avenue, Bronx, NY 10461.

¹J. Warman, M. T. Jahn, and Y. H. Kao, *J. Appl. Phys.* **42**, 5194 (1971).

²For earlier experimental work, see, for example, R. B. Goldfarb, A. F. Clark, A. I. Braginski, and A. J. Panson, *Cryogenics* **27**, 475 (1987); T. Ishida and H. Mazaki, *Jpn. J. Phys.* **26**, L1296 (1987); D.-X. Chen, R. B. Goldfarb, J. Nogues, and K. V. Rao, *J. Appl. Phys.* **64**, 2533 (1988).

³For a review of theoretical work, see, for example, K.-H. Müller, in *Magnetic Susceptibility of Superconductors and Other Spin Systems*, edited by R. A. Hein, T. L. Francavilla, and D. H. Liebenberg (Plenum, New York, 1992).

⁴K. H. Müller, *Physica C* **159**, 717 (1989).

⁵L. Ji *et al.*, *Phys. Rev. B* **40**, 10936 (1989).

⁶T. Ishida and R. B. Goldfarb, *Phys. Rev. B* **41**, 8937 (1990).

⁷S. F. Wahid *et al.*, *Physica C* **184**, 88 (1991).

⁸C. D. Jeffries, *et al.*, *Phys. Rev. B* **37**, 9840 (1988).

⁹A. Shaulov *et al.*, *Phys. Rev. B* **43**, 3760 (1991).

¹⁰Y. B. Kim, C. F. Hempstead, and A. R. Strnad, *Phys. Rev. Lett.* **9**, 306 (1962); *Phys. Rev.* **129**, 528 (1963); P. W. Anderson, *Phys. Rev. Lett.* **9**, 309 (1962); P. W. Anderson and Y. B. Kim, *Rev. Mod. Phys.* **36**, 39 (1964).

¹¹C. Y. Lee, L. W. Song, and Y. H. Kao, *Physica C* **191**, 429 (1992); C. Y. Lee, Ph.D. thesis, SUNY, Buffalo, 1993.

¹²Y. Xin *et al.*, *Physica C* **184**, 185 (1991).

¹³J. R. Clem, *Physica C* **153-155**, 50 (1988).

¹⁴L. G. Neumann and Y. H. Kao, *Physica* **108B**, 979 (1981).

¹⁵J. Jung, I. Isaac, and M. A-K. Mohamed, *Phys. Rev. B* **48**, 7526 (1993).

¹⁶J. E. Evetts and B. A. Glowacki, *Cryogenics* **28**, 641 (1988).

¹⁷P. Levy, H. Ferrari, V. Bekeris, and C. Acha, *Physica C* **214**, 111 (1993).

¹⁸Q. H. Lam and C. D. Jeffries, *Physica C* **194**, 47 (1992).